PLOS ONE

Dynamics of water conveying zinc oxide through divergent-convergent channels with the effect of nanoparticles shape when Joule dissipation are significant

Umair Rashid[1], Azhar Iqbal[2]*, Haiyi Liang[1,3]*, Waris Khan[4], Muhammad Waqar Ashraf[2]

1 CAS Key Laboratory of Mechanical Behavior and Design of Materials, Department of Modern Mechanics, University of Science and Technology of China, Hefei, Anhui, China, **2** Mathematics and Natural Sciences, Prince Mohammad Bin Fahd University, Al Khobar, Saudi Arabia, **3** IAT-Chungu Joint Laboratory for Additive Manufacturing, Anhui Chungu 3D Printing Institute of Intelligent Equipment and Industrial Technology, Wuhu, Anhui, China, **4** Department of Mathematics and Statistics, Hazara University, Mansehra, Khyber Pakhtunkhwa, Pakistan

* aiqbal@pmu.edu.sa (AI); hyliang@ustc.edu.cn (HL)

Abstract

Aim of study

The shape effects of nanoparticles are very significant in fluid flow and heat transfer. In this paper, we discuss the effects of nanoparticles shape in nanofluid flow between divergent-convergent channels theoretically. In this present study, various shapes of nanoparticles, namely sphere, column and lamina in zinc oxide-water nanofluid are used. The effect of the magnetic field and joule dissipation are also considered.

Research methodology

The system of nonlinear partial differential equations (PDEs) is converted into ordinary differential equations (ODES). The analytical solutions are successfully obtained and compared with numerical solutions. The Homotopy perturbation method and NDsolve method are used to compare analytical and numerical results respectively.

Conclusion

The results show that the lamina shape nanoparticles have higher performance in temperature disturbance and rate of heat transfer as compared to other shapes of nanoparticles.

1. Introduction

Nowadays, biomedical nanomaterials have achieved significant attention due to their prominent biomedical applications and biological characteristics. The significant development of nanomaterials and metal oxide nanoparticles displays promising and far-ranging prospects for the biomedical field, especially for anticancer gene/drug delivery, antibacterial, biosensing, cell

capacity (J/kg K); P, Density (kg/m^3); ϕ, Solid volume fraction; μ, Dynamic viscosity (N.sm^{-2}); σ^*, Stefan Boltzmann constant (w.m^{-2}. k^{-4}); k^*, Absorption coefficient (m^{-1}); p, pressure; v$_r$, radial velocity; αnf, Thermal diffusivity of the nanofluid (m/s^2); m, Shape variable; n$_f$, Nanofluid; f, Liquid; s, Solid; Ec, Eckert number; M, Hartmann number; Pr, Prandtl number; Re, Reynolds number; α, Divergent-Convergent parameter; B, Electromagnetic induction; σ, Fluid conductivity.

imaging, etc. Jiang et al. [1] and Mishra et al. [2]. Zinc oxide nanoparticles have very important metal oxide nanoparticles, which are employed in varieties of fields because of their chemical and peculiar physical properties [3, 4]. Zinc oxide has excellent antimicrobial, antibacterial and UV blocking properties. Adding Zinc oxide nanoparticles in finished fabrics in the textile industry has exhibited the most attractive function of visible light and ultraviolet resistance, deodorant and bacteria [5]. Due to strong UV absorption properties, Zinc oxide nanoparticles are also used in care products like cosmetics and sunscreen [6]. Zinc oxide is also utilized in other industry fields involving photocatalysis, concrete production, electrotechnology industries, electronics, etc. [4]. The small size of Zinc oxide makes it more convenient to absorb in the body. Thus, commonly nano Zinc oxide is used in the preservation of food. Zinc oxide nanoparticles have gained much consideration in biomedical applications. Zinc oxide nanoparticles relatively less toxic property as compared to other metal oxide nanoparticles. Zinc oxide nanoparticles have a comparatively inexpensive and excellent exhibit in biomedical applications such as antibacterial, anticancer, diabetes treatments, Drug delivery, anti-inflammation, bioimaging and wound healing [1, 2]. The studies about heat transfer in Zinc oxide nanofluids are relatively rare as compared to other metal oxide nanofluids [7].

Magnetohydrodynamics has various applications in industrial and geophysical fields. In the field of fluid mechanics, magnetohydrodynamics is one attractive topic of researchers. Magnetohydrodynamics is applied in plasma generators, Hall acceleration and cooling of nuclear reactors [8]. Many researchers did work on magnetohydrodynamics fluid flow. Makinde et al. [9] discussed a numerical solution of magnetohydrodynamics Casson fluid flow on an upper horizontal thermally stratified surface. Koriko et al. [10] examined the 3-dimensional flow of water conveying alumina and water conveying alumina Iron oxide with the influence of a magnetic field. Tlili et al. [11] analyzed the 3-dimensional magnetohydrodynamics (AA7072 /AA7075) methanol hybrid nanofluid with slip effect. Ashwinkumar [12] studied heat transfer and mass transfer analysis in unsteady magnetohydrodynamics flow of (aluminum alloy and silver) water nanofluid. Samrat et al. [13] analyzed the effect of the chemical reaction and thermal radiation on the 2-dimensional flow of magnetic nanofluid. Mabood et al. [14] studied the boundary layer analysis of 2-dimensional unsteady hybrid nanofluid flow over a flat slendering surface.

Most physical phenomena and scientific problems occur nonlinearly. To obtain the analytical solution of such problems are partially difficult, excluding in limited problems. Recently, several methods have been achieved significant attention such as the variational iteration method [9], Hirota's method [10], Homotopy analysis method [11], homogeneous balance method [12] as well as homotopy perturbation method. The first time, "He" introduced the Homotopy perturbation method (HPM) [15]. The Homotopy perturbation method (HPM) is an efficient and powerful technique to find the solution of nonlinear and linear equations. The homotopy perturbation method (HPM) is a combination of the homotopy and perturbation methods. Homotopy perturbation method (HPM) can take significant advantage of the convectional perturbation method while eliminating its restrictions. The homotopy perturbation method (HPM) has been most successfully applied by many authors to solve several types of nonlinear and linear equations in engineering and science [16]. Homotopy perturbation method (HPM) is applied by many researchers to handle varieties of engineering and scientific applications to solve several function equations. The solution of Homotopy perturbation method is supposed as a sum of an infinite series which converges quickly to exact solutions. Many researchers have been conducted their research by applying Homotopy perturbation method (HPM) to the nonlinear and linear equations [17].

Jeffery [18] and Hamel introduced a fluid flow which is known as Jeffery Hamel flow. It is a two-dimensional flow between two parallel walls. Jeffery Hamel flow is caused by a sink or

Table 1. Thermophysical properties of zinc oxide(ZnO) and water as [23, 24].

Physical properties	Zinc oxide	Pure water
ρ (kg/m3)	5600	997.1
Cp (J/kg K)	495.2	4179
k (W/m K)	13	0.60

source at the intersection of channel walls. Analysis of Jeffery Hamel flow, mass transfer and heat transfer of fluid between divergent and convergent channels are very important motive [19]. The flow between divergent and convergent is very significant due to its uses in industries, medical, engineering and biomechanics. Various researchers have been tried to extend the flow in converging and diverging channels by considering the impact of different parameters such as slip, magnetohydrodynamic and heat transfer phenomena. Change in angle, it makes a significant role in these flow as discussed in several studies [20]. Sheikholeslami discussed MHD Jeffery Hamel nanofluid flow analytically in the non-parallel wall [21]. Ochieng et al. [22] examined the Jeffery and Hamel flow with nonlinear skin friction and viscosity flow through a divergent conduit in the existence of a magnetic field. Nehad et al. [23] discussed that the Nusselt number proportional to the heat transfer is ascertained at the higher value of suction and stretching ratio the water conveying multiple wall CNT and silicon dioxide.

It is a necessity to find heat transfer under the exact shape of nanoparticles. The shape effect of zinc oxide nanoparticles in Gold-hybrid nanofluid has been discussed by Dinarvand and Rostami [24]. However, the shape effects of zinc oxide nanoparticles in nanofluid water base between non-parallel walls have not been addressed previously. The present study aims to discuss the zinc oxide nanoparticles shapes effects between non-parallel. Furthermore, the results of the Homotopy perturbation method are compared with NDsolve technique and have been reported in the literature to check the reliability and validity of the Homotopy perturbation method.

2. Mathematical formulation

In this report, the problem of steady, two-dimension and incompressible nanofluid flow between divergent-convergent channels is considered. Furthermore, it has also considered that flow is uniform along the z-axis and the velocity of nanofluid is radial. It also considers that the velocity of nanofluid is dependent on r and θ coordinates. The magmatic field applied transverse to the diction of flow. The equations of the problem are modeled as [25]. Thermophysical properties of zinc oxide (ZnO) and water are presented in Table 1. The values of nanoparticles shape factor are presented in Table 2.

$$\frac{\rho_{n_f}}{r}\frac{\partial}{\partial r}(r.v_r) = 0, \tag{1}$$

$$v_r\frac{\partial v_r}{\partial r} = -\frac{1}{\rho_{n_f}}\frac{\partial p}{\partial r} + v_{n_f}\left[\frac{\partial^2 v_r}{\partial r^2} + \frac{1}{r}\frac{\partial v_r}{\partial r} + \frac{1}{r^2}\frac{\partial^2 v_r}{\partial \theta^2} - \frac{v_r}{r^2} - \frac{\sigma B^2 v_r}{\rho_{n_f} r^2}\right], \tag{2}$$

Table 2. Shape factor parameters of nanoparticles [26].

Shapes	column	sphere	lamina
ϕ	0.4710	1	0.1857
m	6.3698	3	16.1576

$$-\frac{1}{\rho_{n_f}r}\frac{\partial p}{\partial \theta} + 2\frac{v_{n_f}}{r^2}\frac{\partial v_r}{\partial \theta} = 0, \tag{3}$$

$$(\rho Cp)_{nf}v_r\frac{\partial T}{\partial r} = k_{n_f}\left[\frac{1}{r}\frac{\partial}{\partial r}\left(r\frac{\partial T}{\partial r}\right) + \frac{1}{r^2}\frac{\partial^2 T}{\partial \theta^2}\right] + u_{n_f}\left[2.\left(\left(\frac{\partial v_r}{\partial r}\right)^2 + \left(\frac{v_r}{r}\right)^2\right) + \left(\frac{1}{r}\frac{\partial v_r}{\partial r}\right)^2\right]$$

$$+ \frac{\sigma B^2 v_r}{r^2}, \tag{4}$$

where p, v_r, T, B, σ denote the pressure, radial velocity, temperature, electromagnetic induction and fluid conductivity, respectively. Also u_{n_f}, v_{n_f}, ρ_{n_f}, k_{nf}, Cp_{nf} denote the dynamic viscosity, kinematic viscosity, density, thermal conductivity and heat capacity of nanofluid, respectively.

The boundary conditions of the problem are

$$V_r = V_{max}, \frac{\partial v_r}{\partial \theta} = 0, \frac{\partial T}{\partial \theta} = 0 \ at \ \theta = 0$$

$$V_r = 0, T = T_w \ at \ \theta = \alpha \tag{5}$$

T_w denote the wall temperature.

For radial motion

$$f(\theta) = r.V_r$$

The variables are considered as [25]

$$\mathrm{f}(\eta) = \frac{f(\theta)}{f_{max}}, \ \mathrm{g}(\eta) = r^2.\frac{T}{T_w}, \ \eta = \frac{\theta}{\alpha} \tag{6}$$

where f_{max} denote the central line of momentum. Substituting Eq (6) into Eqs (2–4) and eliminating P, we get

$$f'''' - 2Re\alpha[BS]ff' + (4 - B.M)\alpha^2 f' = 0, \tag{7}$$

$$g'' + 4\alpha^2 g + 2\alpha^2\frac{Y}{H}Prfg + \frac{PrEc}{ReBH}(4\alpha^2\mathrm{f}^2 + f'^2) + \frac{PrEcM}{H}\mathrm{f}^2 = 0 \tag{8}$$

In this study we consider as

$$S = (1 - \phi) + \frac{\rho_s}{\rho_f}\phi, B$$

$$= (1 - \phi)^{2.5}, Y = (1 - \phi) + \frac{(\rho Cp)_s}{(\rho Cp)_f}\phi, H = \frac{[k_s + (m-1)k_f] - (m-1)\phi(k_f - k_s)}{[k_S + (m-1)k_f] + \phi(k_f - k_s)} \tag{9}$$

Where ϕ, subscript f and subscript s denote the nanofluid volume fraction, base fluid and solid nanoparticle respectively.

Also

$Re = \frac{af_{max}}{v}$ is Reynolds number, $Pr = \frac{(\rho Cp)_f f_{max}}{k_f}$ Prandtl number, $Ec = \frac{a^2 f_{max}^2}{(Cp)_f T_w}$ is Eckert number and $M = \sqrt{\frac{\sigma B^2}{v_f \rho_f}}$ is Hartmann number.

The Boundary value conditions of problems are

$$f(0) = 1, f'(0) = 0, f(1) = 0, g'(0) = 0, g(1) = 1.$$

The physical quantity Nusselt number is given by

$$r^2 Nu_r = H.\left[2 - \frac{g'(1)}{\alpha}\right] \tag{10}$$

3. Homotopy perturbation method

In order to obtain the analytical solution, the homotopy pertutbation method is simulate non-linear ordinary differential Eqs (7 and 8). The solution of Eqs (7 and 8) by applying the Homotopy perturbation method we conduct as follows:

$$(1 - P)(f''' - f_0''') + P(f''' - 2Re\alpha BSff' + (4 - BM)\alpha^2 f') = 0 \tag{11}$$

$$(1 - P)\left(g'' - g''_0\right) + P\left(g'' + 4\alpha^2 g + 2\alpha^2 \frac{Y}{H} Pr fg + \frac{PrEc}{ReBH}\left(4\alpha^2 f^2 + f'^2\right) + \frac{PrEcM}{H} f^2\right) = 0 \tag{12}$$

We consider f and g in the following form

$$f = f_0 + pf_1 + p^2 f_2 \dots\dots\dots\dots\dots\dots\dots\dots \quad .. \tag{13}$$

$$g = g_0 + pg_1 + p^2 g_2 \dots\dots\dots\dots\dots\dots\dots\dots \tag{14}$$

Assuming $f_0''' = 0$ and $g_0'' = 0$ substituting f and g from Eqs (13) and (14) into Eqs (11) and (12) respectively. Also, some arrangement and simplification based on powers of p term we have

$$p^0: \qquad f_0''' = 0 \tag{15}$$

$$f_0(0) = 1, f_0'(0) = 0, f_0(1) = 0 \tag{16}$$

$$p^1: \qquad f_1'''' + 2Re\alpha BSf_0 f_0' + (-BM + 4)\alpha^2 f_0 = 0 \tag{17}$$

$$f_1(0) = 0, f_1'(0) = 0, f_1(1) = 0 \tag{18}$$

$$p^2: \qquad f_2''' + 2Re\alpha BSf_0 f_1' + 2Re\alpha BSf_1 f_0' + (-BM + 4)\alpha^2 f_1' = 0 \tag{19}$$

$$f_2(0) = 0, f_2'(0) = 0, f_2(1) = 0 \tag{20}$$

$$p^0: \qquad g_0'' = 0 \tag{21}$$

$$g_0'(0) = 0, g_0(1) = 1 \tag{22}$$

$$p^1: \qquad g_1'' + 4\alpha^2 g_0 + \frac{2\alpha^2 Y f_0 Pr g_0}{H} + \frac{PrEc(4\alpha^2 f_0^{\,2} + f_0'2)}{ReHB} + \frac{PrEcMf_0^{\,2}}{H} = 0 \tag{23}$$

$$g_1'(0) = 0, g_1(1) = 0 \tag{24}$$

$$p^2: \qquad g_2'' + 4\alpha^2 g_1 + \frac{2\alpha^2 Y f_0 Pr g_1}{H} + \frac{2\alpha^2 Y f_1 Pr g_0}{H} + \frac{PrEc(8\alpha^2 f_0 f_1 + 2f_0' f_1')}{RHB} + \frac{2PrEcMf_0 f_1}{H}$$
$$= 0 \tag{25}$$

$$g_2'(0) = 0, g_2(1) = 0$$

Solving Eqs (15–25) with boundary values conditions we have

$$f_0(\eta) = -\eta^2 + 1 \tag{26}$$

$$f_1(\eta) = -2\alpha\left(\frac{1}{60} BReS\eta^6 + \frac{1}{24}(\alpha BM - 2BReS - 4\alpha)\eta^4\right)$$
$$+ \frac{1}{2}\left(\frac{1}{6}\alpha^2 BM - \frac{4}{15}\alpha BReS - \frac{2}{3}\alpha^2\right)\eta^2 \tag{27}$$

$$f_2(\eta) = -\frac{1}{30}\Big(A^2\Big(\frac{B^2 Re^2 S^2 \eta^{10}}{45} + \frac{(36AB^2 ReSM - 72B^2 Re^2 S^2 - 144ABReS)\eta^8}{336}\Big)$$

$$+ \frac{(10A^2 B^2 M^2 - 60AB^2 ReSM + 72B^2 Re^2 S^2 - 80A^2 BM + 240ABReS + 160A^2)\eta^6}{120}$$

$$+ \frac{(-5A^2 B^2 M^2 + 18AB^2 ReSM - 16B^2 Re^2 S^2 + 40A^2 BM - 72ABReS - 80A^2)\eta^4}{24}\Big)^2$$

$$+ \frac{\left(-\frac{1}{120}A^4 B^2 M^2 + \frac{1}{42}A^3 B^2 ReSM - \frac{163}{9450}A^2 B^2 Re^2 S^2 + \frac{1}{15}A^4 BM - \frac{2}{21}A^3 BReS - \frac{2}{15}A^4\right)\eta^2}{2} \tag{28}$$

$$f = -\frac{1}{360}\Big((\eta - 1)\Big(360 + \frac{4A^2 B^2 Re^2 S^2 \eta^8}{15} + \frac{9BReA^2\big((BM - 4)A - \frac{242BReS}{135}\big)S\eta^6}{7} + \Big((BM - 4)^2 A^3 - \frac{33BReS(BM - 4)A^2}{7}\Big) +$$

$$\frac{514AB^2 Re^2 S^2}{105} + 12BReS)A\eta^4 + \frac{514AB^2 Re^2 S^2}{105} + 12BReS)A\eta^4 \tag{29}$$

$$g_0(\eta) = 1 \tag{30}$$

$$g_1(\eta) = \frac{1}{ReHB}\Big(Pr\Big(-\frac{1}{30}BEcMRe\eta^6 + \frac{1}{6}A^2 BReY\eta^4 - \frac{2}{15}A^2 Ec\eta^6 + \frac{1}{6}BEcMRe\eta^4 - A^2 BReY\eta^2 + \frac{2}{3}A^2 Ec\eta^4$$

$$-\frac{1}{2}BEcMRe\eta^2 - 2A^2Ec\eta^2 - \frac{1}{3}\eta^4Ec)) - 2\eta^2A^2 +$$

$$\frac{(25A^2YPrReB + 60A^2ReHB + 11PrEcMReB + 44A^2EcPr + 10PrEc)}{30ReHB} \tag{31}$$

$$g_2(\eta) = \frac{1}{30H^2ReB}\left(A\left(-\frac{1}{45}B^2ECHMPrRe^2S\eta^{10} + \frac{1}{28}A^2B^2HPrRe^2SY\eta^8 - \frac{4}{45}A^2BECHPrReS\eta^{10}\right.\right.$$

$$-\frac{1}{45}ABECMPr^2ReY\eta^{10} - \frac{5}{56}AB^2ECHM^2PrRe\eta^8 + \frac{3}{7}ABECHMPrRe\eta^8$$

$$+\frac{1}{6}A^3B^2HMPrReY\eta^6 -$$

$$110A^3Y\eta^2PrHReB - \frac{7}{3}A^3BPr^2ReY^2\eta^6 + \frac{55}{6}A^3BPr^2ReY^2\eta^4 - 25A^3BPr^2ReY^2\eta^2$$

$$+\frac{95}{3}A^3BHPrReY\eta^4$$

$$+\frac{4}{3}A^3BEcHMPr\eta^6 - \frac{5}{3}A^3BEcHMPr\eta^4 + \frac{5}{3}ABEcHMPr\eta^4 - \frac{3}{7}PrRe\eta^8SHBEc - 20PrEcA\eta^2H$$

$$+\frac{5}{28}A^3BPr^2ReY^2\eta^8 - 2ABECHMPrRe\eta^6 - 11ABECMPr^2ReY\eta^2 + \frac{20}{3}ABECHMPrRe\eta^4 -$$

$$\frac{5}{12}AB^2EcHM^2PrRe\eta^4 - \frac{12}{5}A^2BEcHPrReS\eta^6 + \frac{1}{3}AB^2EcHM^2PrRe\eta^6 - \frac{8}{3}BEcHPrReS\eta^4$$

$$+\frac{6}{7}A^2BEcHPrReS\eta^8 + \frac{2}{3}A^2B^2HPrRe^2SY\eta^4 - \frac{4}{3}ABECMPr^2ReY\eta^6\frac{5}{12}A^3B^2HMPrReY\eta^4$$

$$-\frac{5}{14}A^3BEcHMPr\eta^2 - \frac{16}{3}A^3BHPrReY\eta^6 - \frac{4}{3}ABECHMPr\eta^6 - \frac{4}{45}A^3ECPr^2Y\eta^{10}$$

$$+\frac{12}{7}A^3ECHPr\eta^8$$

$$-\frac{5}{14}AEcPr^2Y\eta^8 + 20A^3BH^2Re\eta^4 + \frac{20}{3}AEcHPr\eta^6 + \frac{6}{7}A^3EcPr^2Y\eta^8 - \frac{16}{3}A^3EcPr^2Y\eta^6$$

$$+\frac{52}{3}A^3EcPr^2Y\eta^4 + \frac{2}{3}AEcPr^2Y\eta^6 - 44A^3EcPr^2Y\eta^2 + \frac{5}{3}AEcPr^2Y\eta^4 - 10AEcPr^2Y\eta^2)$$

$$-652B^2EcHMPrRe^2S + 1740A^3BEcHMPr + 210840A^3BHPrReY - 2608A^2BEcHPrReS +$$

$$19676ABEcMPr^2ReY - 652B^2EcHMPrRe^2S + 1740A^3BEcHMPr + 210840A^3BHPrReY -$$

$$2608A^2BEcHPrReS + 19676ABEcMPr^2ReY + 20220AEcPr^2Y + 50400AEcHP \tag{32}$$

$$g = \frac{1}{75600BH^2Re}\Big(450(\eta+1)A^2Y\big(2Y\big(\eta^6 - \frac{181}{15}\eta^4 + \frac{589}{15}\eta^2 - \frac{1511}{15}\big)B - $$

$$\frac{112\big(\eta^8 - \frac{121}{14}\eta^6 + \frac{719}{14}\eta^4 - \frac{2011}{14}\eta^2 + \frac{4919}{14}\big)Ec}{225}\big)A^2$$

$$-\frac{28\big(MRe\big(\eta^8 - \frac{121}{14}\eta^6 + \frac{719}{14}\eta^4 - \frac{2011}{14}\eta^2 + \frac{4919}{14}\big)B + \frac{225\eta^6}{14} - \frac{195\eta^4}{14} - \frac{1245\eta^2}{14} + \frac{5055}{14}\big)Ec}{225}\Big)$$

$$(\eta-1)Pr^2 + 420(\eta)+1)H(MReY)\big(\eta^4 - \frac{3}{2}\eta^2 - \frac{3}{2}\big)B^2$$

$$+\big(-\frac{15M\eta^6 Ec}{7} + \big(\frac{41MEc}{7} - 32ReY\big)\eta^4$$

$$+\big(-\frac{29MEc}{7} + 158ReY\big)\eta^2 - \frac{29MEc}{7} - 502ReY\big)B + \frac{72\big(\eta^6 - \frac{11}{3}\eta^4 + \frac{107}{9}\eta^2 - \frac{355}{9}\big)Ec}{7}\big)A^4$$

$$- 502ReY\big)B$$

$$+\frac{3BS\big(ReY\big(\eta^6 - \frac{25}{3}\eta^4 + \frac{31}{3}\eta^2 + \frac{31}{3}\big)B - \frac{112\big(\eta^8 - \frac{121}{14}\eta^6 + \frac{257}{14}\eta^4 - \frac{163}{14}\eta^2 - \frac{163}{14}\big)Ec}{45}\big)ReA^3}{14}+$$

$$+\big(-\frac{15M^2\big(\eta^6 - \frac{41}{15}\eta^4 + \frac{29}{15}\eta^2 + \frac{29}{15}\big)EcReB^2}{28} + \big(\frac{18MRe\eta^6 Ec}{7} - \frac{66M\big(Re + \frac{28}{33}\big)Ec\eta^4}{7} +$$

$$\big(\big(\frac{214}{7}MRe + 2M\big)Ec + 30ReY\big)\eta^2 + \big(2M - \frac{710}{7}MRe\big)Ec - 150ReY\big)B$$

$$+ 16Ec(\eta^4 + 6\eta^2 - 24))A^2$$

$$-\frac{2BS\big(MRe\big(\eta^8 - \frac{121}{14}\eta^6 + \frac{257}{14}\eta^4 - \frac{163}{14}\eta^2 - \frac{163}{14}\big)B + \frac{135\eta^6}{7} - \frac{705\eta^4}{7} + \frac{135\eta^2}{7} + \frac{135}{7}\big)EcReA}{15} - 6(MRe(\eta^4$$

$$-4\eta^2) + 11)B + 10\eta^2$$

$$+ 10Ec\big((\eta-1)Pr + 50400B\big(\frac{3}{2} + (\eta^4 - 6\eta^2 + 5)A^4 + (-3\eta^2 + 3)A^2\big)H^2Re\big) \qquad (33)$$

4. Result and discussion

In this section, nanofluid flow and heat transfer between divergent-convergent channels with nanoparticles shapes effects are discussed. Also, the results obtained by using Homotopy perturbation are clarified with the numerical NDsolve method. Geometry of the problem is presented in Fig 1. The results of the comparative solutions are shown in Figs 2 and 3. Fig 4 displays the variation in the velocity of ZnO-water nanofluid within divergent-convergent channels under the influences of ϕ. From Fig 4, it is also noted that the velocity of nanofluid decreases with increase ϕ in a divergent channel but an opposite behaviour is found in the convergent channel. The effects of α on the velocity of nanofluid are shown in Fig 5. It is also observed from Fig 5 that the velocity of nanofluid has an inverse relation within the divergent channel but direct relation within the convergent channel.
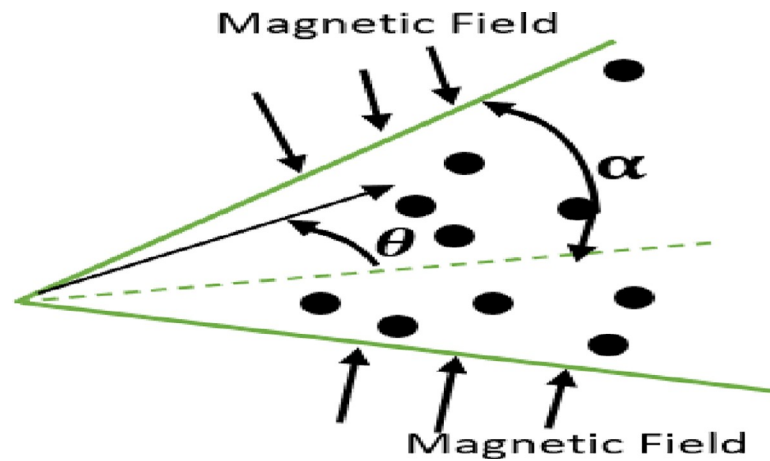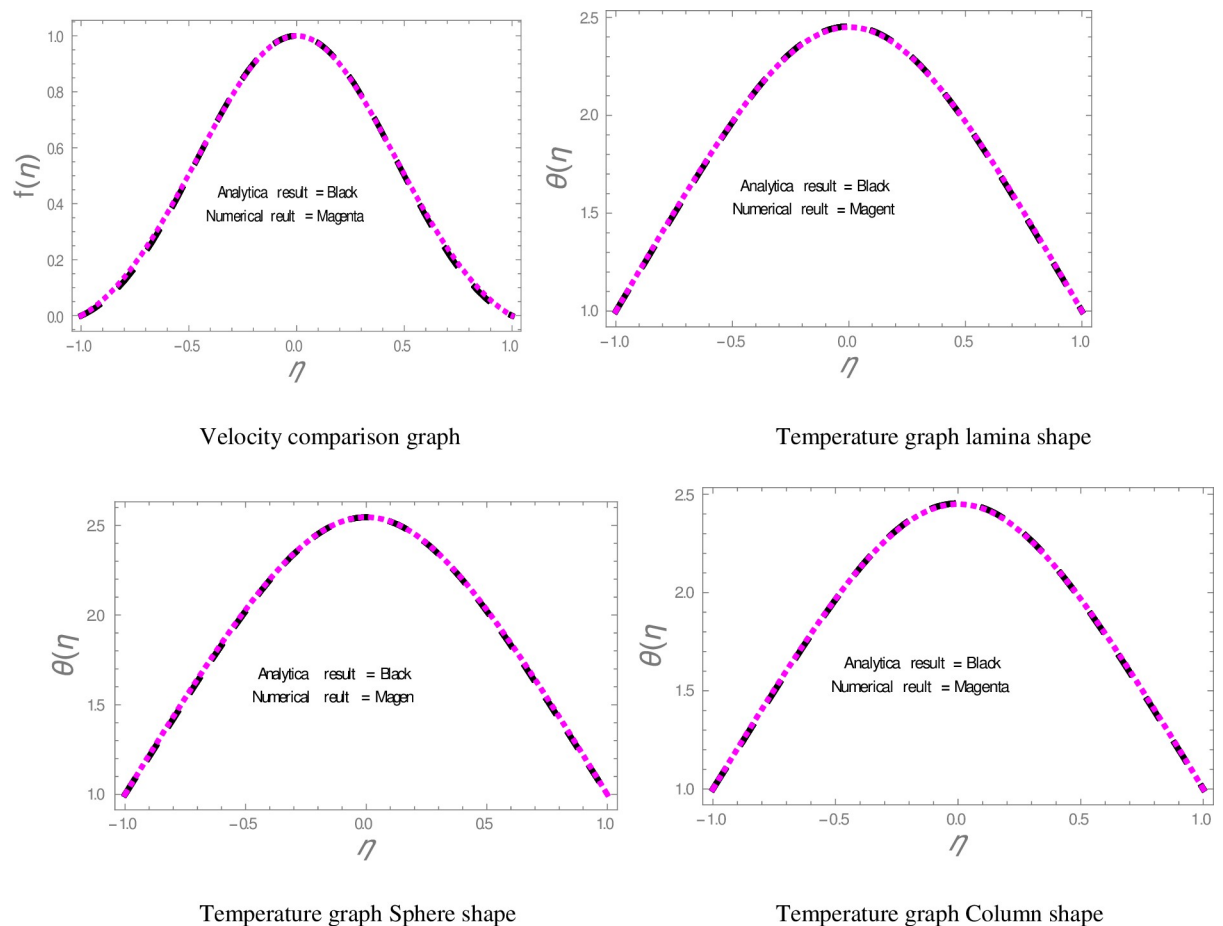
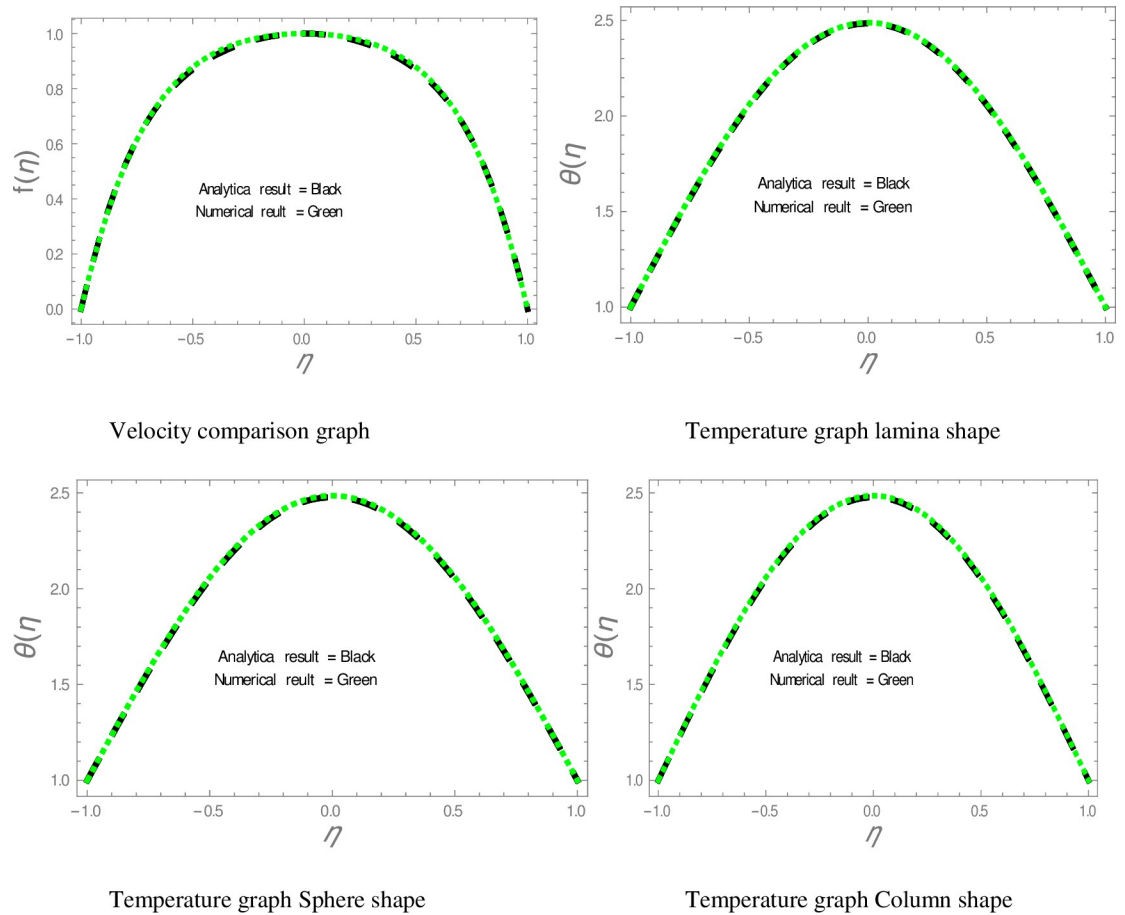**Fig 1. Geometry of the problem.**

The effect of shape factor on the temperature within divergent-convergent channels is presented in Fig 6. Fig 6 illustrates that sphere shape nanoparticles have higher, whereas lamina shape nanoparticles have lower performance in temperature disturbance within divergent-convergent channels. Fig 7 presents the variation in temperature profile with the influences of

Velocity comparison graph

Temperature graph lamina shape

Temperature graph Sphere shape

Temperature graph Column shape

Fig 2. Comparison of results in diverging channel.

Velocity comparison graph

Temperature graph lamina shape

Temperature graph Sphere shape

Temperature graph Column shape

Fig 3. Comparison of results in converging channel.
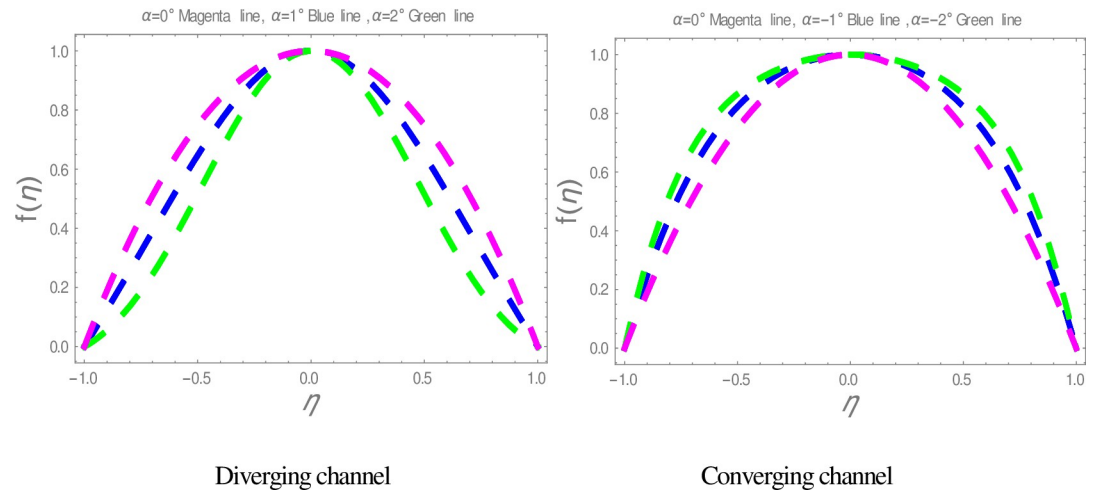
https://doi.org/10.1371/journal.pone.0245208.g003

ϕ. It is observed in Fig 7 that the temperature of nanofluid is a decreasing function of solid volume fraction within divergent-convergent channels. It is also noted from Fig 7 that the performance of sphere shape nanoparticles in temperature profile is higher than column and lamina

Diverging channel

Converging channel

Fig 4. The effect of ϕ on velocity graphs.

https://doi.org/10.1371/journal.pone.0245208.g004

$\alpha=0°$ Magenta line, $\alpha=1°$ Blue line, $\alpha=2°$ Green line

$\alpha=0°$ Magenta line, $\alpha=-1°$ Blue line, $\alpha=-2°$ Green line
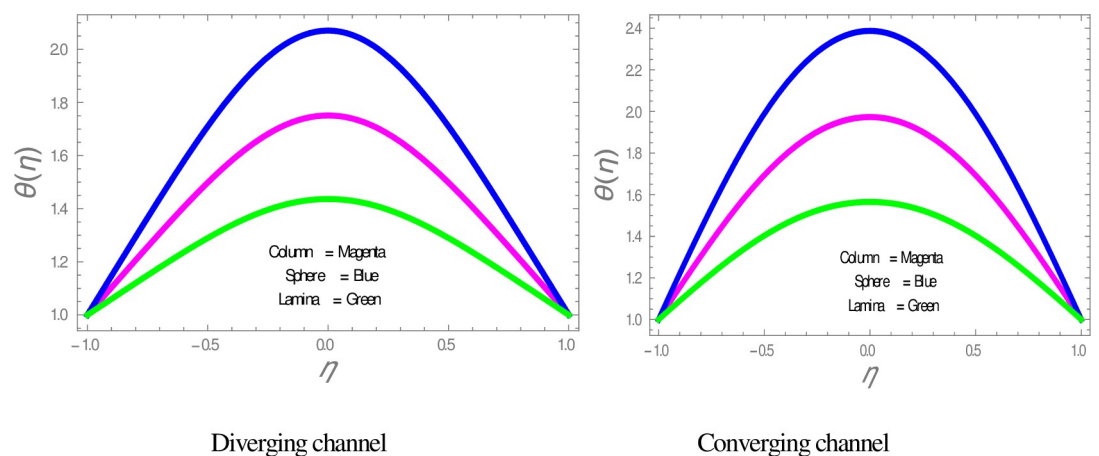
Diverging channel

Converging channel
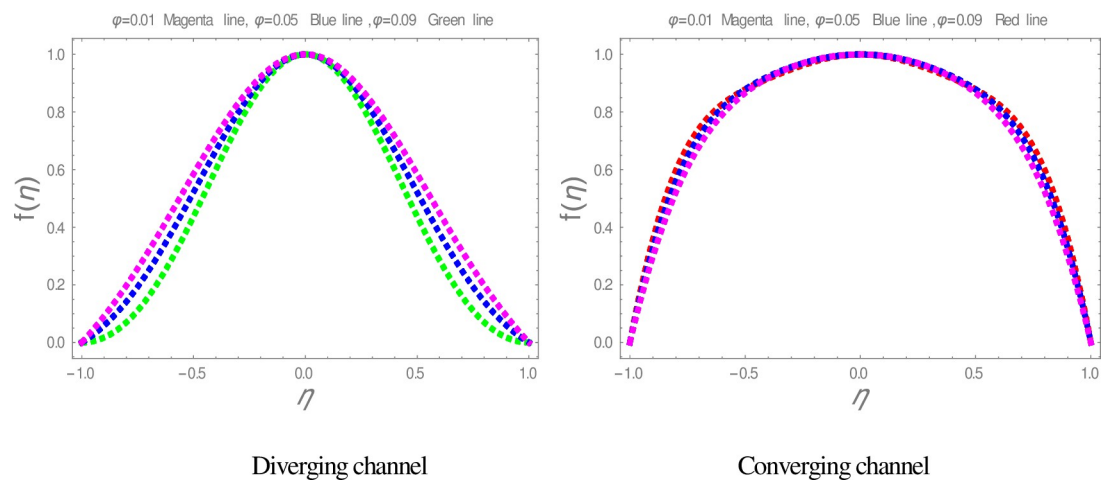
Fig 5. The effect of α on velocity graphs.

nanoparticles within divergent-convergent channels. Fig 8 depicts the behaviors of α in the temperature profile. The temperature of nanofluid has a decreasing function of α in the divergent channel, while an opposite result has found in the convergent channel.

Fig 9 is plotted to check the effect of M on temperature profile. The figure illustrates that the temperature of nanofluid within divergent-convergent channels has a direct relation with M. Fig 10 shows the effect of Ec on temperature profile within divergent-convergent channels. Form Fig 10, it is noted that the effect of Ec within divergent channel is similar to the effect of Ec in convergent channel. It is also noted from Figs 9, 10 performance of sphere shape nanoparticles is lower than other shapes of nanoparticles in divergent-convergent channels with the effect of M and Ec. Variation in temperature profile with the influences of Re is presented in Fig 11. It is analyzed from Fig 11, Re has an inverse and direct relation with temperature distribution within the divergent channel and convergent channel, respectively. The performance of nanoparticles is similarly examined with the impacts of M and Ec. Figs 12, 13 are sketched to investigate the heat transfer rate. From Figs 12, 13, we observe that the heat transfer rate in lamina shape nanoparticles is better than other nanoparticles shapes. The comparison of

Column = Magenta
Sphere = Blue
Lamina = Green

Column = Magenta
Sphere = Blue
Lamina = Green

Diverging channel

Converging channel

Fig 6. The effect of particles on temperature profiles.

Diverging channel   Converging channel
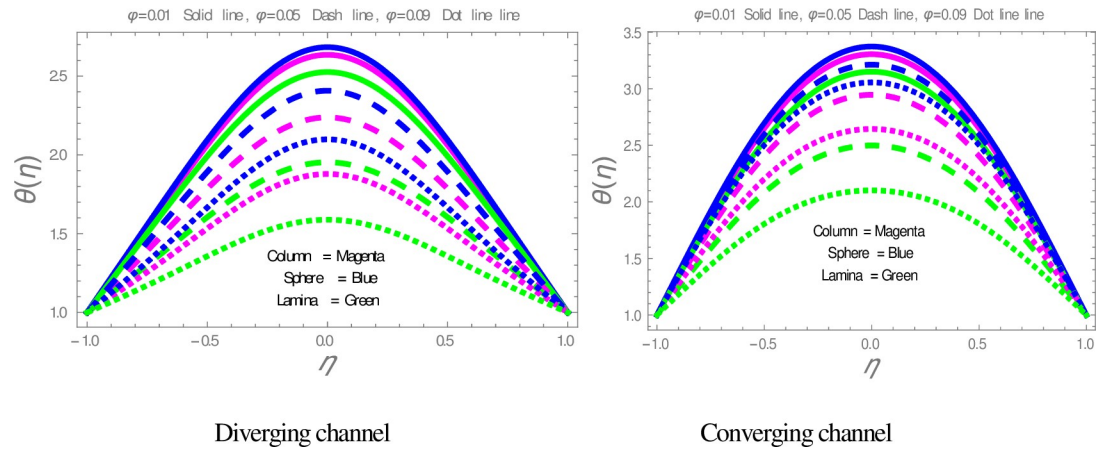
Fig 7. The effect of ϕ on the temperature profile.

homotopy perturbation method and NDsolve solutions are presented in Table 3. Table 4 Shows comparison of solution with already published paper.

5. Conclusion

The effects of nanoparticle shapes (sphere, column and lamina) in a dynamic of water conveying Zinc oxide through divergent-convergent channels are computed by using analytical and numerical techniques. The effect of the magnetic field and joule dissipation are also examined. A fixed value of Pr = 6.2 is used in this study. Apropos to the above discussion, the following dedications are pointed below:

- The sphere shape nanoparticles have a greater role in temperature distribution and the lowest role in heat transfer.

- The lamina shape nanoparticles have a greater role in heat transfer and the lowest role in temperature distribution

- The column shape nanoparticles have a middle role in heat transfer and temperature distribution.

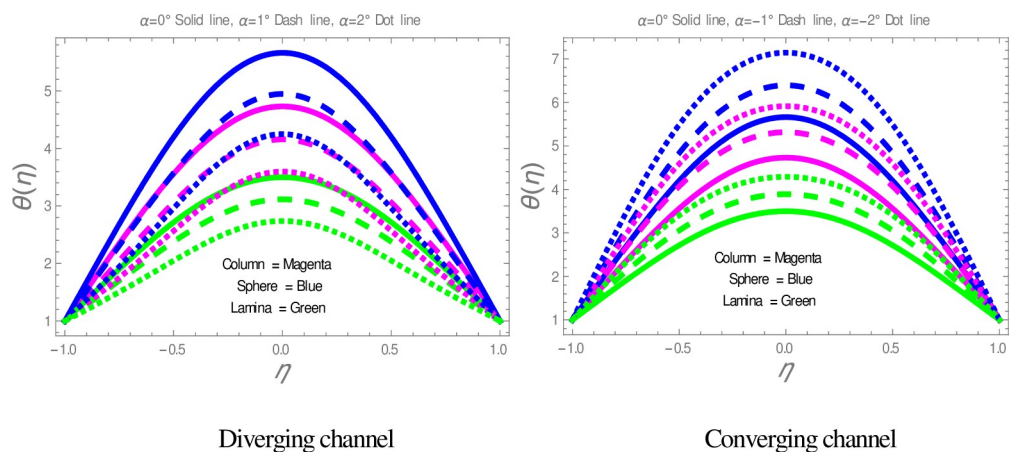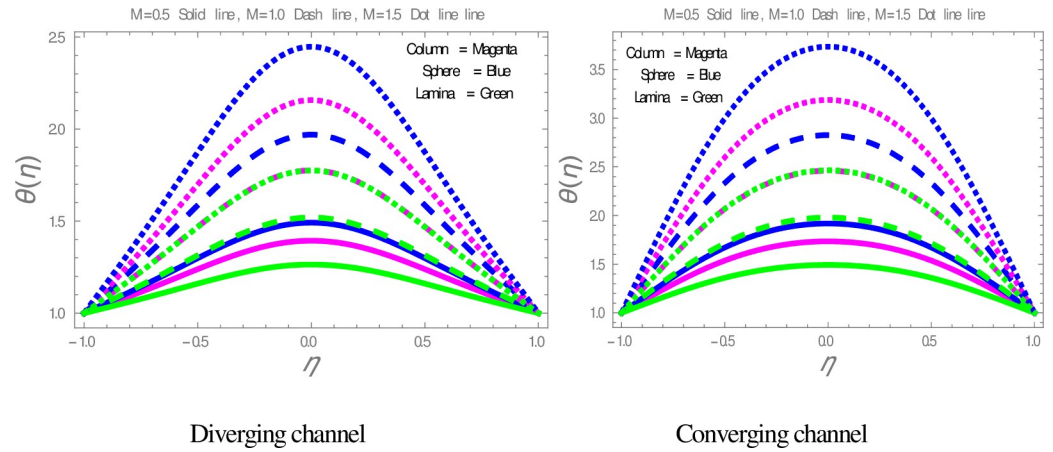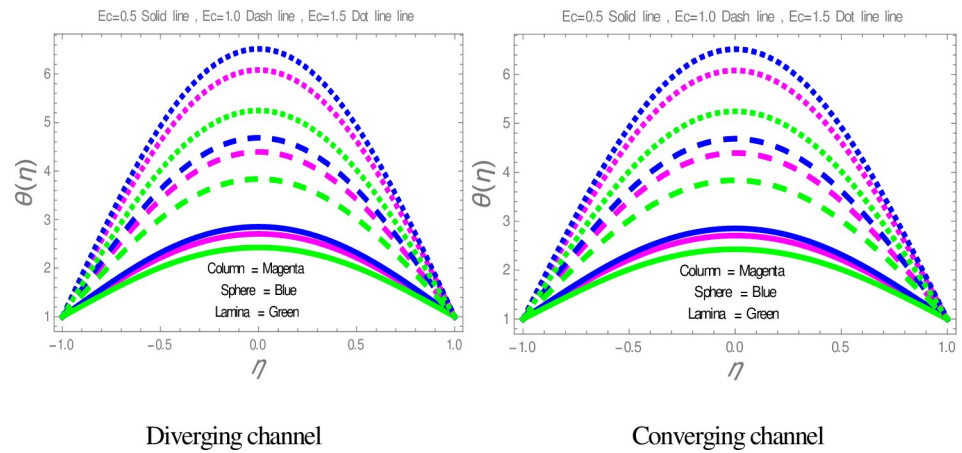Diverging channel   Converging channel

Fig 8. The effect of α on temperature profiles.

Fig 9. The effect of *M* on temperature profiles.

https://doi.org/10.1371/journal.pone.0245208.g009

Fig 10. The effect of *Ec* on temperature profiles.

https://doi.org/10.1371/journal.pone.0245208.g010
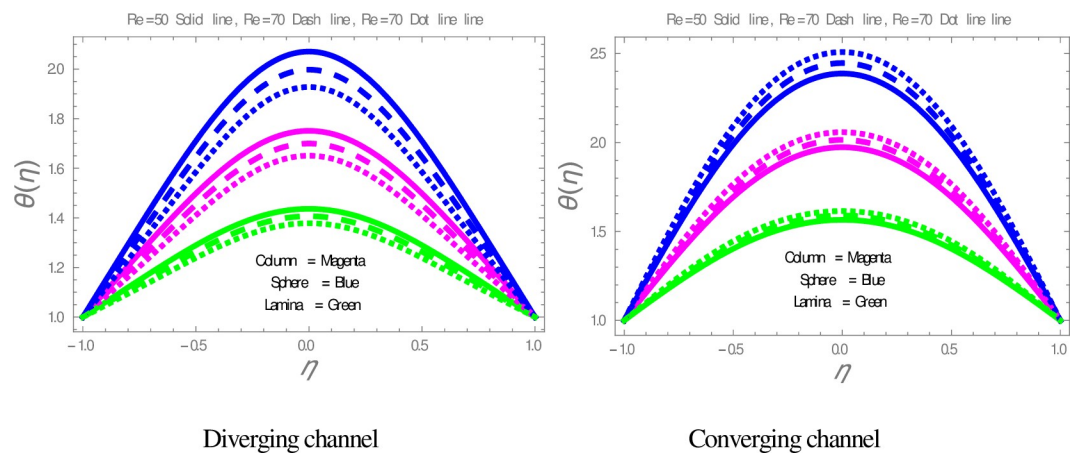
Fig 11. The effect Re on temperature profiles.

https://doi.org/10.1371/journal.pone.0245208.g011

Diverging channel   Converging channel
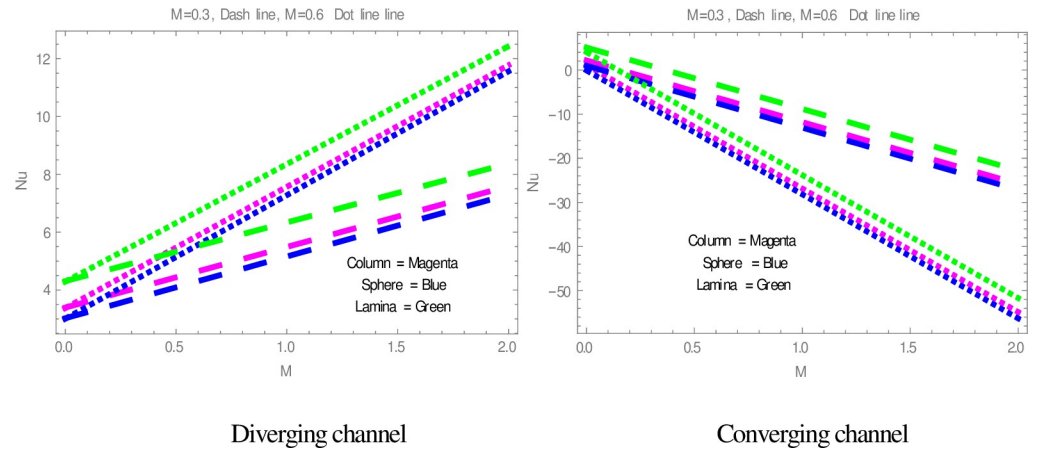
Fig 12. The effect of M on heat transfer.

Diverging channel   Converging channel
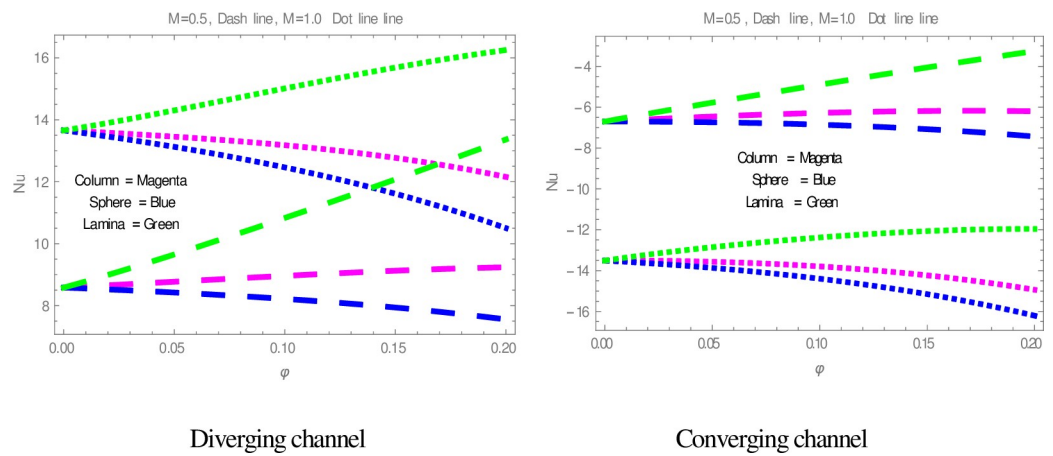
Fig 13. The effect of ϕ on heat transfer.

Table 3. Comparison of values for $\phi = 0.2$, $M = 1.0$, $R_e = 2.0$ and $\alpha = 0$.

x	$f(x)$	$f(x)$	$f'(x)$	$f'(x)$
	ND	HPM	ND	HPM
1	0.9900	0.9900	-0.2000	-0.2000
2	0.9600	0.9600	-0.4000	-0.4000
3	0.9099	0.9099	-0.6000	-0.6000
4	0.8400	0.8400	-0.8000	-0.8000
5	0.7500	0.7500	-1.0000	-1.0000
6	0.6400	0.6400	-1.2000	-1.2000
7	0.5100	0.5100	-1.4000	-1.4000
8	0.3600	0.3600	-1.6000	-1.6000

Table 4. Comparison of results with already published work [27].

Re	Convergent channel Abbasbandy and Shivanian Results	Convergent channel Present Results (HPM)	Diverging channel Abbasbandy and Shivanian Results	Diverging channel Present Results (HPM)
10	1.7845468	1.7848768	2.2519486	2.2515638
20	1.5881535	1.5882108	2.5271922	2.5243141
30	1.4136920	1.4139204	2.8326293	2.8332759
40	1.2589939	1.2595367	3.1697121	3.1720138
50	1.219890	1.1229166	3.5394156	3.5456609
60	1.0007429	1.0019168	3.9421402	3.9563603
80	0.7985672	0.7982056	4.8450718	4.8974887

https://doi.org/10.1371/journal.pone.0245208.t004

Author Contributions

Conceptualization: Umair Rashid.

Formal analysis: Umair Rashid, Azhar Iqbal, Haiyi Liang, Waris Khan, Muhammad Waqar Ashraf.

Investigation: Azhar Iqbal, Haiyi Liang, Waris Khan, Muhammad Waqar Ashraf.

Methodology: Umair Rashid, Azhar Iqbal, Waris Khan.

Software: Umair Rashid.

Supervision: Haiyi Liang.

Validation: Umair Rashid, Haiyi Liang.

Visualization: Umair Rashid, Haiyi Liang.

Writing – original draft: Umair Rashid.

Writing – review & editing: Umair Rashid, Azhar Iqbal, Haiyi Liang, Waris Khan, Muhammad Waqar Ashraf.

References

1. Jiang J, Pi J, Cai J. The Advancing of Zinc Oxide Nanoparticles for Biomedical Applications. 2018;2018.

2. Mishra PK, Mishra H, Ekielski A, Talegaonkar S, Vaidya B. Zinc oxide nanoparticles: a promising nanomaterial for biomedical applications. Drug Discov Today. 2017; 22: 1825–1834. https://doi.org/10.1016/j.drudis.2017.08.006 PMID: 28847758

3. Press D. Titanium dioxide and zinc oxide nanoparticles in sunscreens: focus on their safety and effectiveness. 2011; 95–112.

4. Ruszkiewicz AJA, Pinkas A, Ferrer B, Peres T V, Tsatsakis A, Aschner M. Neurotoxic effect of active ingredients in sunscreen products, a contemporary review. Toxicol Reports. 2017. https://doi.org/10.1016/j.toxrep.2017.05.006 PMID: 28959646

5. Hatamie A, Khan A, Golabi M, Turner APF, Beni V, Mak WC, et al. Zinc Oxide Nanostructure-Modified Textile and Its Application to Biosensing, Photocatalysis, and as Antibacterial Material. Langmuir. 2015; 31: 10913–10921. https://doi.org/10.1021/acs.langmuir.5b02341 PMID: 26372851

6. Newman MD, Stotland M, Ellis JI. The safety of nanosized particles in titanium dioxide- and zinc oxide-based sunscreens. J Am Acad Dermatol. 2009; 61: 685–692. https://doi.org/10.1016/j.jaad.2009.02.051 PMID: 19646780

7. Wing M, Lee T. Numerical Study of Flow and Heat Transfer with ZnO-Water Nanofluid in Flattened Tubes Abstract: 2019; 1–26. https://doi.org/10.1515/cppm-2019-0092

8. Mahanthesh B, Lorenzini G, Oudina FM, Animasaun IL. Significance of exponential space- and thermal-dependent heat source effects on nanofluid flow due to radially elongated disk with Coriolis and Lorentz forces. J Therm Anal Calorim. 2020; 141: 37–44. https://doi.org/10.1007/s10973-019-08985-0

9. Makinde OnE of HT and LFE on the F of MCF over an UHS of a TSMS of a P of RD, Sandeep N, Ajayi TM, Animasaun IL. Numerical Exploration of Heat Transfer and Lorentz Force Effects on the Flow of MHD Casson Fluid over an Upper Horizontal Surface of a Thermally Stratified Melting Surface of a Paraboloid of Revolution. Int J Nonlinear Sci Numer Simul. 2018; 19: 93–106. https://doi.org/10.1515/ijnsns-2016-0087

10. Koriko OK, Adegbie KS, Animasaun IL, Ijirimoye AF. Comparative Analysis Between Three-Dimensional Flow of Water Conveying Alumina Nanoparticles and Water Conveying Alumina–Iron(III) Oxide Nanoparticles in the Presence of Lorentz Force. Arab J Sci Eng. 2020; 45: 455–464. https://doi.org/10.1007/s13369-019-04223-9

11. Tlili I, Nabwey HA, Ashwinkumar GP, Sandeep N. 3-D magnetohydrodynamic AA7072-AA7075/methanol hybrid nanofluid flow above an uneven thickness surface with slip effect. Sci Rep. 2020; 10: 1–14. https://doi.org/10.1038/s41598-020-61215-8 PMID: 32144369

12. Ashwinkumar GP. Heat and mass transfer analysis in unsteady MHD flow of aluminum alloy/silver-water nanoliquid due to an elongated surface. Heat Transf. 2020. https://doi.org/10.1002/htj.21947

13. Samrat SP, Sulochana C, Ashwinkumar GP. Impact of thermal radiation and chemical reaction on unsteady 2D flow of magnetic-nanofluids over an elongated plate embedded with ferrous nanoparticles. Front Heat Mass Transf. 2018; 10. https://doi.org/10.5098/hmt.10.31

14. Mabood F, Ashwinkumar GP, Sandeep N. Simultaneous results for unsteady flow of MHD hybrid nanoliquid above a flat/slendering surface. J Therm Anal Calorim. 2020. https://doi.org/10.1007/s10973-020-09943-x

15. He JH. Addendum: New interpretation of homotopy perturbation method. Int J Mod Phys B. 2006; 20: 2561–2568. https://doi.org/10.1142/S0217979206034819

16. Reshmi B. Application of homotopy perturbation method to Poisson equation. 2008; 37: 119–123.

17. Fereidoon A, Yaghoobi H, Davoudabadi M. Application of the Homotopy Perturbation Method for Solving the Foam Drainage Equation. 2011; 2011. https://doi.org/10.1166/jbn.2011.1319 PMID: 21870458

18. Registered W, Street M. The two- dimensional steady motion of a viscous fluid. 37–41. https://doi.org/10.1080/14786440408635327

19. Khan U, Adnan, Ahmed N, Mohyud-Din ST. Soret and Dufour effects on Jeffery-Hamel flow of second-grade fluid between convergent/divergent channel with stretchable walls. Results Phys. 2017; 7: 361–372. https://doi.org/10.1016/j.rinp.2016.12.020

20. Mohyud-Din ST, Khan U, Hassan SM. Numerical investigation of magnetohydrodynamic flow and heat transfer of copper–water nanofluid in a channel with non-parallel walls considering different shapes of nanoparticles. Adv Mech Eng. 2016; 8: 1–9. https://doi.org/10.1177/1687814016637318

21. Hatami M, Sheikholeslami M, Hosseini M, Ganji DD. Analytical investigation of MHD nanofluid flow in non-parallel walls. J Mol Liq. 2014; 194: 251–259. https://doi.org/10.1016/j.molliq.2014.03.002

22. Oketch Ochieng F. Hydromagnetic Jeffery-Hamel Unsteady Flow of A Dissipative Non-Newtonian Fluid with Nonlinear Viscosity. 2018; 14: 1101–1119. Available: https://pdfs.semanticscholar.org/8ffd/866f64e0c38a61e3f4ada45a4487607099d6.pdf?_ga=2.114667079.1564540523.1585002727-1387465479.1584723840

23. Shah NA, Animasaun IL, Wakif A, Koriko OK, Sivaraj R, Adegbie KS, et al. Significance of suction and dual stretching on the dynamics of various hybrid nanofluids: Comparative analysis between type i and type II models. Phys Scr. 2020; 95: 95205. https://doi.org/10.1088/1402-4896/aba8c6

24. Dinarvand S, Nademi Rostami M. An innovative mass-based model of aqueous zinc oxide–gold hybrid nanofluid for von Kármán's swirling flow: A comprehensive report on effects of nanoparticle shape factor. J Therm Anal Calorim. 2019; 138: 845–855. https://doi.org/10.1007/s10973-019-08127-6

25. Kezzar M, Sari MR, Bourenane R, Rashidi MM, Haiahem A. Heat transfer in hydro-magnetic nanofluid flow between non-parallel plates using DTM. J Appl Comput Mech. 2018; 4: 352–364. https://doi.org/10.22055/JACM.2018.24959.1221

26. Rashid U, Ibrahim A. Impacts of Nanoparticle Shape on Al2O3-Water Nanofluid Flow and Heat Transfer over a Non-Linear Radically Stretching Sheet. Adv Nanoparticles. 2020; 09: 23–39. https://doi.org/10.4236/anp.2020.91002

27. Abbasbandy S, Shivanian E. Exact analytical solution of the MHD Jeffery-Hamel flow problem. Meccanica. 2012; 47: 1379–1389. https://doi.org/10.1007/s11012-011-9520-3